Phase separation in poly(methyl methacrylate)/polycarbonate blends

P. Sakellariou*
ICI Paints, Research Department, Wexham Road, Slough SL5 2DS, UK

and G. C. Eastmond
*Department of Chemistry, Donnan Laboratories, Liverpool University, Liverpool L69 3BX, UK*

This paper deals with the compatibility of a chlorine-containing polycarbonate with poly(methyl methacrylate) (PMMA). The polymer–polymer interaction parameter, χ, has been determined from the experimental phase diagram by means of the Flory–Huggins theory. The interfacial tension, interfacial thickness and interfacial density profile have also been calculated from the experimental value of χ by means of Helfand's mean-field treatment. The calculated interfacial thickness has been compared to experimental data from optical, transmission and scanning electron microscopy.

Introduction

In a series of papers we have discussed the interfacial activity of polycarbonate/poly(methyl methacrylate) (PMMA) graft copolymers in incompatible blends of polycarbonate/PMMA[1–3]. A chlorine-containing polycarbonate (I) was used in these studies.

I
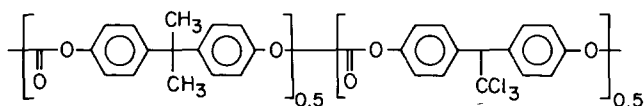
We demonstrated that the copolymer is most active as an interfacial agent when the molecular weight of the copolymer block corresponding to the minor phase was distinctly higher than that of the corresponding homopolymer. Furthermore, copolymer interfacial activity deteriorated as the molecular weight of the same homopolymer increased towards that of the copolymer block. We have argued that the degree of incompatibility between the two homopolymers and between copolymer and homopolymer influences the efficiency of copolymer molecules to create interface by controlling the relative position of the critical concentration for phase separation between homopolymer and copolymer with respect to system binodal. Knowledge of the degree of incompatibility of the homopolymers is, therefore, of great importance.

A significant volume of data is available on the compatibility of bisphenol A polycarbonate and PMMA. Solvent-cast blends[4,5] have been reported as immiscible whilst melt blended ones have been found to be miscible[6]. Recently, Chiou and Barlow[7] found that precipitation-blended systems were compatible. More importantly, they raised the question of the effect of casting solvent

on system compatibility. This has been confirmed by Kym and Saldanham[5] who discussed in some detail the effect of casting conditions on the final film morphology for a variety of solvents. They concluded that final morphology is largely controlled by competition between phase separation and solvent-induced crystallization. The same authors reported the presence of a UCST-type phase diagram[4]. This has recently been corroborated by Nishimito et al.[8] and Butzbach and Wendorff[9].

The chlorine-containing polycarbonate used in this study (I), a random copolymer of the carbonates of bisphenol A and of 4,4'-dihydroxyphenyl(2,2,2-trichloro)ethane, has been shown by Eastmond and co-workers[2,10] to be immiscible with PMMA over the whole range of blend composition by optical microscopy and dynamic mechanical techniques. Phase separation in solvent-cast blends has been argued to be incomplete, with the segregation of the two components strongly dependent upon casting conditions. This behaviour was explained in terms of deviation from the equilibrium thermodynamics during solvent casting.

We now report quantitative information on the immiscibility of PMMA with the chlorine-containing polycarbonate (I) by calculating the Flory–Huggins polymer–polymer interaction parameter (χ_{23}) from the experimental phase diagram. The experimentally determined polymer–polymer interaction parameter is compared to that obtained from a van Laar-type equation using the solubility parameters. The polymer–polymer interaction parameter has been used to calculate the interfacial concentration profile and interfacial tension using a mean-field approach. Finally, the interfacial thickness is compared to experimental information on the blend morphology.

Experimental

Optical microscopy. Samples were thin sections (3–6 μm) cut normal to the bulk film surface. Birefringence, introduced to the polycarbonate-rich phases during

---

microtoming, gave rise to phase contrast. Under these conditions the polycarbonate-rich phases appeared bright whereas the PMMA-rich ones appeared dark.

Electron microscopy. Transmission electron microscopy on ultrathin sections was carried out by means of a Jeol JEM 200B microscope. Ultrathin sections were cut parallel to the bulk film surface by means of a LKB II microtome at room temperature and stained with aqueous ruthenium tetroxide over 2–3 h. Under these conditions the polycarbonate-rich phase appeared dark. Low acceleration voltages (100 kV) were found necessary for improved phase contrast.

Scanning electron microscopy was also used as an auxiliary technique. The polycarbonate-rich phases were etched away from the surface of carefully trimmed sections by alkaline hydrolysis (25% sodium hydroxide solution). The etched surface was coated with a thin Au/Pt film and viewed under a Philips SEM501 microscope at acceleration voltages of 3 kV and low magnifications to minimize beam damage of the surface.

Ternary phase diagrams. The cloud point curve of PMMA/polycarbonate (I)/dichloromethane ternary system was determined by allowing mixtures of the two polymers in dichloromethane to separate into two layers in tightly sealed tubes in a thermostat (28°C). The position of the interface was monitored over several weeks by means of a cathetometer. Equilibrium was considered to have been attained when the position of the interface did not change over several weeks. After equilibrium had been achieved, the compositions of the two phases were determined by measuring the total solids content of accurately sampled volumes of each phase and the relative contents of the two polymers by means of n.m.r. and u.v. spectroscopy. This procedure allowed determination of tie lines in the phase diagram. Additional points on the binodal were obtained by titrating cloudy solutions of the two polymers in dichloromethane until a clear homogeneous mixture was observed.

Materials. PMMA, obtained from RAPRA, had a molecular weight of $\overline{M}_n = 48.8$ kg mol^{-1} and $\overline{M}_n/\overline{M}_n = 2.5$. The chlorine-containing polycarbonate (I) was prepared by polycondensation of bisphenol A and 4,4′-dihydroxyphenyl(2,2,2-trichloro)ethane as described elsewhere[2]. Its molecular weight was 20.2 kg mol^{-1}. Polymer molecular weights were determined by means of gel permeation chromatography (g.p.c.) with tetrahydrofuran (THF) as the carrier and with respect to polystyrene calibration.

Film preparation. Samples were prepared by solution casting from dilute solutions (4% w/v) in dichloromethane. Dichloromethane is a good solvent for both components and will not, therefore, be expected to induce phase separation during film casting. Blend composition was kept constant at 65/35 w/w PMMA/polycarbonate. The casting procedure has been discussed in detail in an earlier report[2].

Results and discussion of phase separation thermodynamics

The compatibility of the system can be predicted by means of the Hildebrand–Scatchard solubility theory[11]. The enthalpic contribution of the polymer–polymer interaction parameter can be expressed in terms of the

cohesive energy density difference between the two polymers:

$$\chi_{23} = \frac{V_r}{RT}(\delta_2 - \delta_3)^2 \tag{1}$$

where V_r is the reference volume.

The calculated polymer–polymer interaction parameter can then be compared to the critical value predicted by the Flory–Huggins theory:

$$(\chi_{23})_{cr} = 0.5(x_{n2}^{-1/2} + x_{n3}^{-1/2})^2 \tag{2}$$

where x_n is the number average degree of polymerization.

This scheme is a qualitative prediction for polymer compatibility and is expected to be successful only in the absence of strong specific interactions. The solubility parameters for PMMA and our polycarbonate were calculated (*Table 1*) by means of the new correlation values for the cohesive energy and the V_g group contribution parameters[12]. The reference volume was taken conveniently as 100 cm^3 mol^{-1} as suggested by Krause[13]. This does not introduce any significant errors in terms of the qualitative nature of the approach. If indeed V_r were assigned the value of PMMA (86.5 cm^3 mol^{-1}) the prediction would remain the same qualitatively. Strong incompatibility was predicted for the system as the polymer–polymer interaction parameter (0.101) exceeded the critical value (0.014) by approximately one order of magnitude. This is in agreement with the experimental evidence presented in earlier reports[10].

Despite the successful application of the aforementioned qualitative scheme, it is important to be able to determine the polymer–polymer interaction parameter experimentally. This is particularly important in view of the reported compatibility between poly(epichlorohydrin) and poly(ε-caprolactone) through specific interactions[14] involving chlorine and carbonyl groups. The Flory–Huggins polymer–polymer interaction parameter in solution can be calculated from the three tie-lines (*Figure 1*) of the experimental phase diagram[15–17].

The Gibbs free energy of mixing two polymers in the presence of a solvent (ΔG_m) is given by the Flory–Huggins equation:

$$\frac{\Delta G_m}{RT} = (n_1 \ln \phi_1 + n_2 \ln \phi_2 + n_3 \ln \phi_3)$$

$$+ (\chi_{12}\phi_1\phi_2 + \chi_{13}\phi_1\phi_3 + \chi_{23}\phi_2\phi_3)$$

$$\times (m_1 n_1 + m_2 n_2 + m_3 n_3) \tag{3}$$

where n_i and ϕ_i denote, respectively, the number of moles and volume fraction of component i. m_i is the ratio of the molar volume of component i to that of the solvent. Subscripts 1, 2 and 3 correspond to the solvent and the two polymers, respectively. The chemical potential of component i is calculated by differentiating the Gibbs free energy with respect to the number of molecules of this component in the system. The chemical potential of

Table 1 Molar volume and solubility parameters for polycarbonate and PMMA

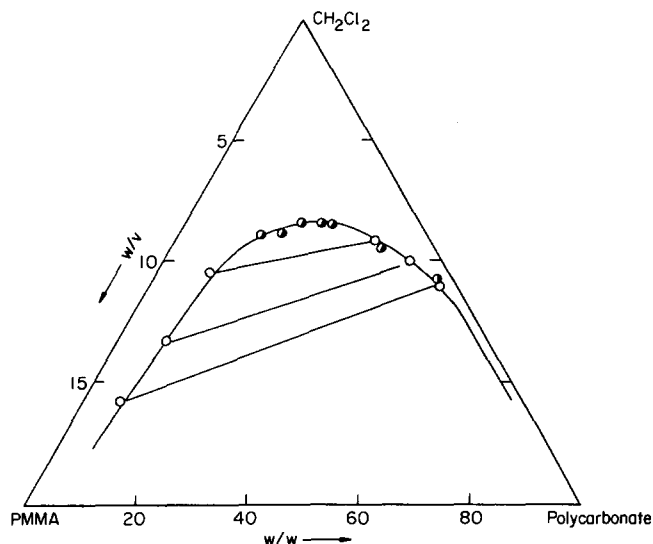| Component	V_g (cm^3 mol^{-1})	δ (cal$^{1/2}$ cm$^{-3/2}$)
Polycarbonate (I)	450.95	9.9
PMMA	86.5	9.1$_2$

Figure 1 Phase diagram of PMMA/polycarbonate (I)/dichloromethane at 28°C

the components in each phase at equilibrium would obey:

$$\mu_i'' = \mu_i' \tag{4}$$

Two equations are obtained for the two phases by introducing the numerical expressions for the chemical potentials for each component in equation (4).

$$\chi_{23}[(\phi_2' - \phi_2'') - (\phi_1'' - \phi_1')] - \chi_{13}[(\phi_2' - \phi_2'') - (\phi_1'' - \phi_1')]$$
$$+ \chi_{12}[(\phi_2' - \phi_2'') + (\phi_1'' - \phi_1')] = \ln(\phi_1''/\phi_1') - m_2^{-1} \ln(\phi_2''/\phi_2') \tag{5}$$

$$\chi_{23}[(\phi_3'' - \phi_3') + (\phi_1'' - \phi_1')] + \chi_{13}[(\phi_3'' - \phi_3') - (\phi_1'' - \phi_1')]$$
$$- \chi_{12}[(\phi_3'' - \phi_3') + (\phi_1'' - \phi_1')] = m_3^{-1} \ln(\phi_3''/\phi_3') - \ln(\phi_1''/\phi_1') \tag{6}$$

The system of equations (5) and (6) can be solved numerically with respect to χ_{12}, χ_{13} and χ_{23} by considering the experimental data for two adjacent tie lines. Narasimhan *et al.*[15,16] suggested that it is reasonable to consider χ_{12} and χ_{13} concentration independent within a narrow concentration range (<0.1). In that case, equations (5) and (6) can be rewritten for two adjacent tie lines (I and II).

$$\chi_{23}^I[(\phi_2' - \phi_2'') - (\phi_1'' - \phi_1')]_I - \chi_{13}^I[(\phi_2' - \phi_2'') - (\phi_1'' - \phi_1')]_I$$
$$+ \chi_{12}^I[(\phi_2' - \phi_2'') + (\phi_1'' - \phi_1')]_I = \ln(\phi_1''/\phi_1')_I - m_2^{-1} \ln(\phi_2''/\phi_2')_I \tag{7}$$

$$\chi_{23}^{II}[(\phi_2' - \phi_2'') - (\phi_1'' - \phi_1')]_{II} - \chi_{13}^{II}[(\phi_2' - \phi_2'') - (\phi_1'' - \phi_1')]_{II}$$
$$+ \chi_{12}^{II}[(\phi_2' - \phi_2'') + (\phi_1'' - \phi_1')]_{II} = \ln(\phi_1''/\phi_1')_{II} - m_2^{-1} \ln(\phi_2''/\phi_2')_{II} \tag{8}$$

$$\chi_{23}^I[(\phi_3'' - \phi_3') + (\phi_1'' - \phi_1')]_I + \chi_{13}^I[(\phi_3'' - \phi_3') - (\phi_1'' - \phi_1')]_I$$
$$- \chi_{12}^I[(\phi_3'' - \phi_3') + (\phi_1'' - \phi_1')]_I = m_3^{-1} \ln(\phi_3''/\phi_3')_I - \ln(\phi_1''/\phi_1')_I \tag{9}$$

$$\chi_{23}^{II}[(\phi_3'' - \phi_3') + (\phi_1'' - \phi_1')]_{II} + \chi_{13}^{II}[(\phi_3'' - \phi_3') - (\phi_1'' - \phi_1')]_{II}$$
$$- \chi_{12}^{II}[(\phi_3'' - \phi_3') + (\phi_1'' - \phi_1')]_{II} = m_3^{-1} \ln(\phi_3''/\phi_3')_{II} - \ln(\phi_1''/\phi_1')_{II} \tag{10}$$

This is a system of four equations with four unknowns

$(\chi_{12}, \chi_{13}, \chi_{23}^I$ and $\chi_{23}^{II})$ which we have solved numerically using Gaussian elimination. Parameters m_2 and m_3 were calculated from the molar volumes of polycarbonate (I), PMMA and dichloromethane. *Table 2* lists the calculated values for the interaction parameters. In agreement with earlier observations[15-17], the polymer–solvent parameters were greater than 0.5 and have to be rejected. Perhaps this reflects the generally acknowledged inadequacy of the simple Flory–Huggins theory for treating polymer–solvent systems. The polymer–polymer interaction parameters were positive, indicating immiscibility. They increased with decreasing total polymer volume fraction in agreement with earlier observations[15-17]. It would be interesting to compare the calculated values in solution to that corresponding to the plait point of the phase diagram and that predicted for the bulk polymer. The polymer interaction parameter at the plait point $(\chi_{23,pl})$ is given by equation (11):

$$\chi_{23,pl} = \tfrac{1}{2}(m_2^{-1/2} + m_3^{-1/2})^2(1 - \phi_{1,pl})^{-1} \tag{11}$$

A value of 0.08 was calculated from equation (11) for $\chi_{23,pl}$.

We can now estimate the interfacial thickness and the interfacial tension using Helfand's mean-field treatment[18-20]. The interfacial thickness, a_I, is given by:

$$a_I = 2b/(6\chi)^{1/2} \tag{12}$$

where b is the monomer unit effective length and was taken as the geometric mean of the two polymers. For our system it was calculated to be 6.4 Å. *Table 3* compares the interfacial thickness of our system to that reported for polystyrene (PS)/polybutadiene (PB)[20].

The interfacial tension between the two polymers is given by:

$$\gamma_{23} = (\chi/6)^{1/2} b\rho_0 kT \tag{13}$$

where ρ_0 is the monomer number density, taken as $10^{-2} \times L(\text{cm}^{-3})$, where L is Avogadro's number. *Table 3* compares the interfacial tension at room temperature of our system to that of PS/PMMA. The polymer–polymer interaction parameter at room temperature for this system was calculated from the equation given by Russell *et al.*[21]. Both interfacial thickness and interfacial tension suggest that the polycarbonate/PMMA system is more compatible than the PS/PMMA one. This is in agreement with dynamic mechanical and TEM data[22].

Table 2 Polymer–polymer and polymer–solvent interaction parameters calculated for the experimental phase diagram of *Figure 1*

Component 1	Component 2	χ	ϕ_1
Polycarbonate (I)	PMMA	0.029	0.925
Polycarbonate (I)	PMMA	0.021	0.915
Polycarbonate (I)	CH_2Cl_2	0.579	–
PMMA	CH_2Cl_2	0.605	–

Table 3 Interfacial thickness (a_I) and interfacial tension (γ_{23}) of polycarbonate (I)/PMMA, PS/PMMA and PS/polybutadiene (PB) blends at room temperature

System	χ_{23}	a_I (Å)	b (Å)	γ_{23} (dyn cm^{-1})
Polycarbonate/PMMA	0.02	38	6.4	0.9
PS/PB	0.03^a	30^a	(6.4)	(1.1)
PS/PMMA	0.04	25	6.5	1.4

^{a} Reported in reference 21. Values in brackets calculated

Finally, the interfacial concentration profile of polycarbonate homopolymer in the blend can be calculated with lattice models for polymer–polymer interfaces[23,24]:

$$\phi_2(z) = \tfrac{1}{2}(\phi_2^\alpha + \phi_2^\beta) + \tfrac{1}{2}(\phi_2^\alpha - \phi_2^\beta)\tanh(2z/a_i) \qquad (14)$$

where ϕ_2 is the polycarbonate homopolymer volume fraction; superscripts α and β denote the matrix and the dispersed phase, respectively, and z is distance from the interface. Approximate values for polycarbonate volume fraction in the two phases were calculated from dynamic mechanical spectra reported earlier[1,2,22] for this blend using the Fox equation. The interfacial thickness (*Table 3*) was computed from the experimental data using equation (12). *Figure 2* illustrates the polycarbonate density profile calculated from the experimental data. *Figure 3* illustrates the morphologies of a 65/35 w/w PMMA/polycarbonate (I) blend cast from dilute solutions in dichloromethane. Although the resolution of microscopic techniques employing selective etching or staining is not satisfactory for quantitative study of polymer–polymer interfaces, it is reasonable to suggest that the observed morphologies are largely consistent with the theoretical calculations in terms of the presence of a relatively sharp interface. In addition to experimental limitations, non-equilibrium conditions prevailing in the solvent-cast films and the polydispersity of the polymers would account for the observed relative broadening of the interfacial region.

Summary

Consecutive tie lines of the experimental phase diagram of the ternary system polycarbonate (I)/PMMA/dichloromethane have been used to compute the polymer–polymer interaction parameter, χ_{23}. The calculated χ_{23} values have been compared to that calculated from a van Laar-type expression based on the Hildebrand solubility parameters. In agreement with literature data, the experimental values were lower than the predicted ones.

The experimentally determined value of χ_{23} afforded calculation of fundamental parameters of the blend interface including the interfacial tension, the interfacial density profile and the interfacial thickness by means of Helfand's mean-field approach. Experimental morphologies were largely consistent with the theoretical predictions in terms of the presence of relatively sharp interfaces. The
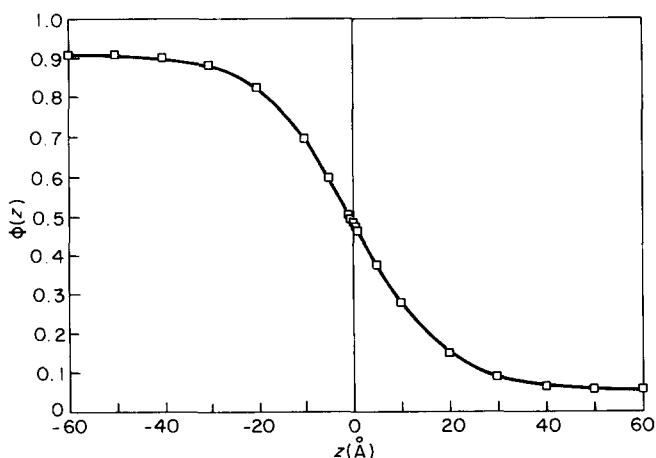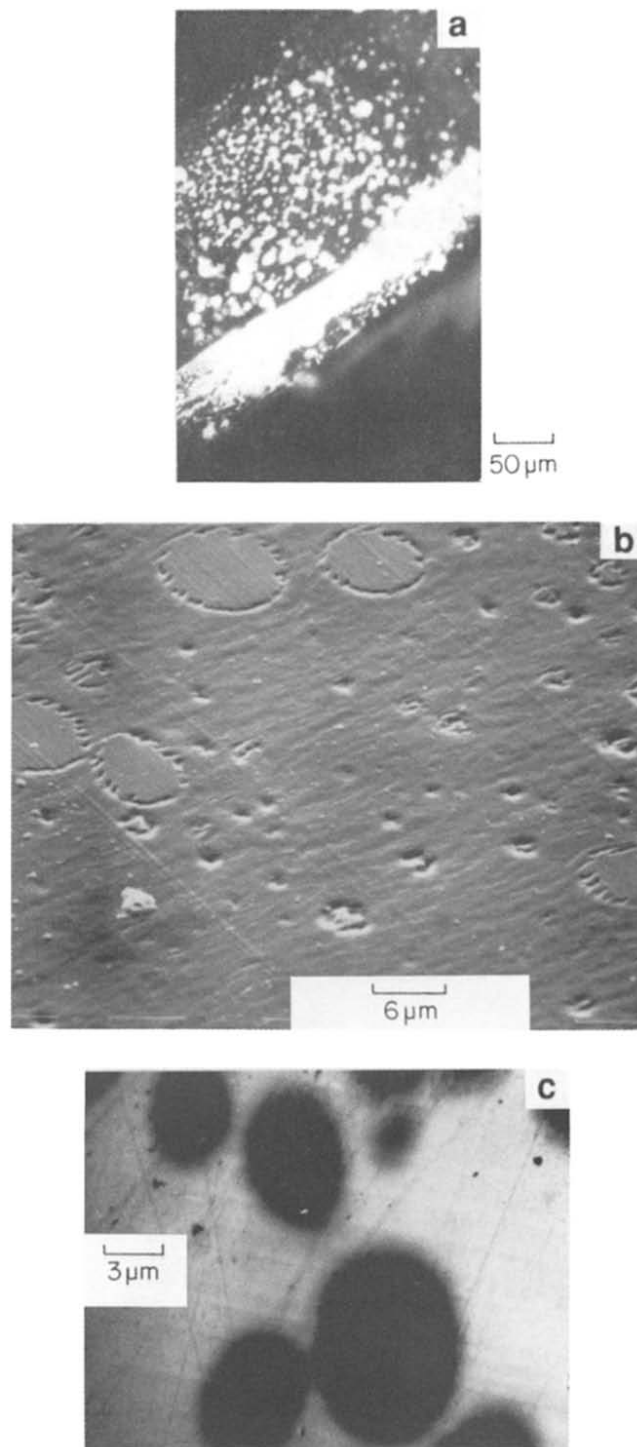

Figure 3 Morphology of PMMA/polycarbonate (I) 65/35 w/w. (a) Optical microscopy; (b) SEM; (c) TEM

relative broadening of the experimental interfaces with respect to the mean-field prediction was attributed to non-equilibrium conditions prevailing in our samples and the polydispersity of our polymers.

References

1   Eastmond, G. C., Jiang, M. and Malinconico, M. *Br. Polym. J.* 1987, **19**, 275
2   Sakellariou, P., Eastmond, G. C. and Miles, I. S. *Polymer* 1991, **32**, 2351
3   Sakellariou, P., Eastmond, G. C. and Miles, I. S. *Polymer* 1992, **33**, 4493
4   Kym, T. and Saldanham, J. M. *J. Polym. Sci., Part C: Polym. Lett.* 1988, **26**, 33

Figure 2 Interfacial density profile of PMMA/polycarbonate (I) 65/35 w/w blend calculated from equation (14)

5   Kym, T. and Saldanham, J. M. *Macromolecules* 1987, **20**, 2840
6   Gardlund, Z. G. in 'Polymer Blends and Composites in Multiphase Systems' (Ed. C. D. Ham), ACS No. 206, Washington, D.C., 1984, Ch. 9, p. 129
7   Chiou, J. S. and Barlow, J. W. *J. Polym. Sci., Polym. Phys. Edn* 1983, **24**, 1161
8   Nishimoto, M., Keskkula, H. and Paul, D. R. *Polymer* 1991, **32**, 1275
9   Butzbach, G. D. and Wendorff, J. H. *Polymer* 1991, **32**, 1155
10 Eastmond, G. C., Jiang, M. and Malinconico, M. *Polymer* 1983, **24**, 1161
11 Hildebrand, J. H., Prausnitz, J. M. and Scott, R. L. in 'Regular and Related Solutions', Van Nostrand Reinhold, Princeton, NJ, 1970
12 Van Krevelen, D. W. in 'Properties of Polymeric Materials', Elsevier, Amsterdam, 1972
13 Krause, S. in 'Polymer Blends' (Eds D. R. Paul and S. Newman), Vol. 1, Academic Press, New York, 1978
14 Fernadez, A. C., Barlow, J. W. and Paul, D. R. *J. Appl. Polym. Sci.* 1984, **29**, 1971
15 Narasimhan, V., Huang, R. Y. M. and Burns, C. M. *J. Polym. Sci., Polym. Symp.* 1986, **74**, 265
16 Narasimhan, V., Huang, R. Y. M. and Burns, C. M. *J. Appl. Polym. Sci.* 1989, **37**, 1909
17 Sakellariou, P. and Rowe, R. C. *J. Appl. Polym. Sci.* 1991, **43**, 845
18 Helfand, E. and Takami, Y. *J. Polym. Sci., Polym. Lett. Edn* 1971, **9**, 741
19 Helfand, E. and Takami, Y. *J. Chem. Phys.* 1971, **56**, 3592
20 Helfand, E. and Takami, Y. *J. Chem. Phys.* 1972, **57**, 1812
21 Russell, T. P., Hjelm, R. P. and Seeger, P. A. *Macromolecules* 1990, **23**, 890
22 Sakellariou, P., Eastmond, G. C. and Miles, I. S. unpublished data
23 Helfand, E. *J. Chem. Phys.* 1975, **63**, 2192
24 Roe, R.-J. *J. Chem. Phys.* 1975, **62**, 490